

## Bifurcation of inter-spike-intervals of a chaotic spiking oscillator with piecewise constant characteristics

Tomonari Hasegawa<sup>†</sup>, Yusuke Matsuoka<sup>†</sup> and Toshimichi Saito<sup>†</sup>

<sup>†</sup>EECE Dept., HOSEI University, Tokyo, 184-0002 Japan, tomonari AT nonlinear.k.hosei.ac.jp

**Abstract**—This paper studies a chaotic spiking oscillator consisting of two capacitors, two signum shape voltage-controlled current sources and one impulsive switch. The vector field of circuit equation is piecewise constant and trajectory is piecewise linear. The circuit exhibits a variety of spike-trains. We study interesting bifurcation of inter-spike-intervals.

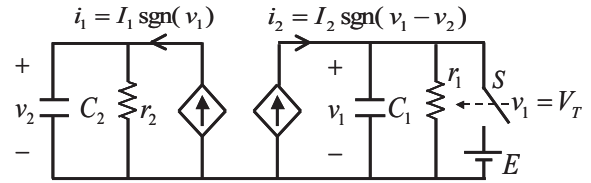


Figure 1: PWC chaotic spiking oscillator.

### 1. Introduction

This paper studies a simple chaotic spiking oscillator (ab. CSO) with piecewise constant (PWC) characteristics [1]. The CSO consists of two capacitors, two signum shape voltage-controlled current sources (VCCSs) and an impulsive switch. If a capacitor voltage reaches threshold level, the switch resets the voltage to the base level instantaneously and the CSO outputs a spike. The circuit equation and vector field are PWC and the trajectory is piecewise linear (PWL). Using the embedded 1-D map, the dynamics can be analyzed theoretically [1].

First we explain the dynamics of the PWC-CSO. When the switch does not present, the trajectory draws rectangular-spiral divergently in the phase plane. Applying the switching, the PWC-CSO generates chaos. Next we investigate inter-spike-intervals (ISIs) characteristics that are given precisely because of the PWL trajectory. The PWC-CSO exhibits various chaotic spike-trains and interesting bifurcation. ISI distribution becomes wide-band as the base level approaches zero. Increasing the base level from zero, the ISI bifurcation has window like structure. In the window, the ISI distribution has narrow-band.

In general, the CSOs have a simple impulse switching that can cause interesting phenomena, e.g., bifurcations, hyperchaos, synchronization and a variety of spike-trains [2]-[4]. The operation of the switch relates to integrate-and-fire dynamics in artificial neuron models. Using the CSOs, we can consider pulse-coupled neural networks (PCNNs) having applications to the image segmentation [4], [5]. Also, analysis of spike-trains may contribute to classification of nonlinear phenomena and application to spike-train communications and A/D converters [6]-[8]. Analysis of ISI is important for fundamental and practical viewpoints. It should be noted that [1] firstly presents the PWC-CSO, however, [1] has not been discussed ISI characteristics.

### 2. The piecewise constant circuit model

Figure 1 shows the PWC chaotic spiking oscillator consisting of two capacitors, two VCCSs and the switch  $S$  where  $r_1$  and  $r_2$  denote parasitic resistors. Two VCCSs have signum characteristics:

$$\begin{cases} i_1 = I_1 \operatorname{sgn}(v_1), \\ i_2 = I_2 \operatorname{sgn}(v_1 - v_2), \end{cases} \quad \operatorname{sgn}(v) = \begin{cases} 1 & \text{for } v \geq 0, \\ -1 & \text{for } v < 0. \end{cases} \quad (1)$$

First, we consider dynamics in the case where the  $S$  is open all the time. For simplicity, we assume that  $r_1$  and  $r_2$  are large enough and open them. In this case the circuit dynamics is described by Equation (2):

$$\begin{cases} C_1 \frac{dv_1}{dt} = I_2 \operatorname{sgn}(v_1 - v_2), \\ C_2 \frac{dv_2}{dt} = I_1 \operatorname{sgn}(v_1), \end{cases} \quad \text{for } S = \text{off}. \quad (2)$$

where the following conditions are assumed:

$$I_1 > 0, \quad I_2 > 0, \quad C_1 I_1 > C_2 I_2 > 0. \quad (3)$$

This equation defines PWC vector fields divided by two border lines  $v_1 = 0$  and  $v_1 = v_2$ .

We then define operation of the  $S$  as shown in Fig. 2 (a) : if  $v_1$  reaches the threshold voltage  $V_T > 0$  then  $S$  is closed and  $v_1$  is reset to the base voltage  $E < V_T$  and the circuit outputs a spike  $z$ :

$$\begin{aligned} (v_1(t+), v_2(t+)) &= (E, v_2(t)) \quad \text{if } v_1(t) = V_T. \\ z(t) &= \begin{cases} 1, & \text{for } v_1(t+) = V_T, \\ 0, & \text{otherwise.} \end{cases} \end{aligned} \quad (4)$$

For simplicity, we assume that reset of  $v_1$  is instantaneous without delay and continuity property of  $v_2$  is held.

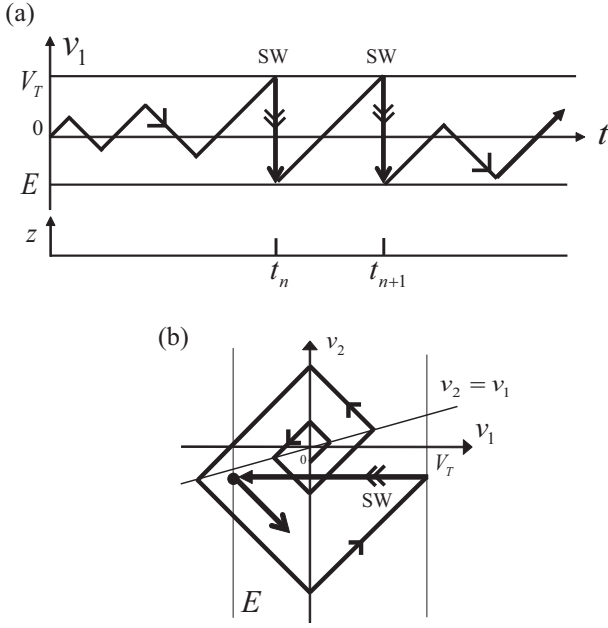


Figure 2: Basic circuit dynamics. (a) Time-domain waveform, (b) Phase plane.

Fig. 2 (b) shows a trajectory in the phase space. Roughly speaking, the instantaneous switching by SW and amplitude increasing by the VCCSs correspond to folding and stretching mechanism to generate chaos, respectively.

In order to analyze the chaotic attractor we normalize the circuit equation. Using the following dimensionless variables and parameters:

$$\tau = \frac{I_2 t}{C_1 V_T}, \quad x = \frac{v_1}{V_T}, \quad y = \frac{v_2}{a V_T}, \quad a = \frac{C_1 I_1}{C_2 I_2}, \quad q = \frac{E}{V_T}.$$

Eqs. (2) and (4) are transformed into Eq. (5):

$$\begin{cases} \frac{dx}{d\tau} = \text{sgn}(x - ay), \\ \frac{dy}{d\tau} = \text{sgn}(x), \end{cases} \quad \text{for } S = \text{off.} \quad (5)$$

$$(x(\tau+), y(\tau+)) = (q, y(\tau)) \quad \text{if } x(\tau) = 1.$$

$$z(\tau) = \begin{cases} 1, & \text{for } x(\tau+) = 1, \\ 0, & \text{otherwise.} \end{cases}$$

It should be noted that this normalized equation is characterized by two parameters  $a$  and  $q$ . Following Condition (3) and  $E < V_T$ , the parameters satisfy

$$a > 1, \quad q < 1. \quad (6)$$

Fig. 3 shows typical chaotic attractors. Roughly speaking, as  $q$  increases from negative to zero, size of chaotic attractor grows ( (a) and (b) ). As  $q$  increases from 0, the switching between  $q$  and 1 becomes frequent ( (c) and (d) ).

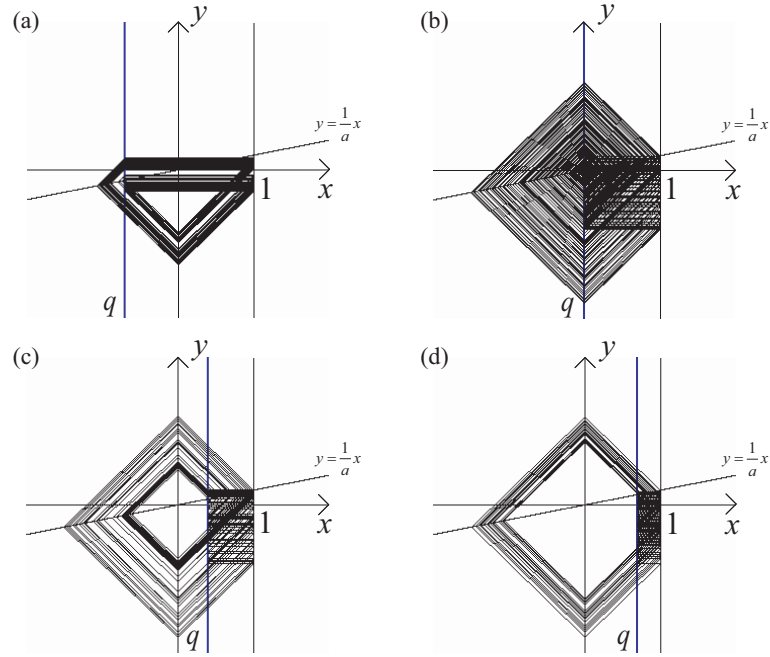


Figure 3: Typical chaotic attractors for  $a = 5$ . ( the border  $y = a^{-1}x$  corresponds to  $v_1 = v_2$  ). (a) Chaotic attractor for  $q = -0.7$ , (b) Chaotic attractor for  $q = 0$ , (c) Chaotic attractor for  $q = 0.4$ , (d) Chaotic attractor for  $q = 0.7$ .

### 3. ISI characteristics

As  $q$  varies, the circuit exhibits interesting bifurcation phenomena of ISI. In order to analyze the phenomena we define switching time  $\tau_n$  as shown in Fig. 4. Let us consider a trajectory started from some point at  $\tau = 0$ . Let  $\tau_1$  denote the first firing time when the trajectory firstly reaches the threshold and is reset to  $q$ . Let  $\tau_n$  denote the  $n$ -th firing time. The  $n$ -th ISI is defined by  $\Delta\tau_n = \tau_{n+1} - \tau_n$ .

Fig. 5 shows histograms of the ISIs corresponding to typical chaotic attractors in Fig. 3. For  $q < 0$  we have observed ISI distribution having narrow band as shown in Fig. 5 (a). As  $q$  increases, the distribution changes to have wide band as shown in Fig. 5 (b). For  $q > 0$ , the trajectory

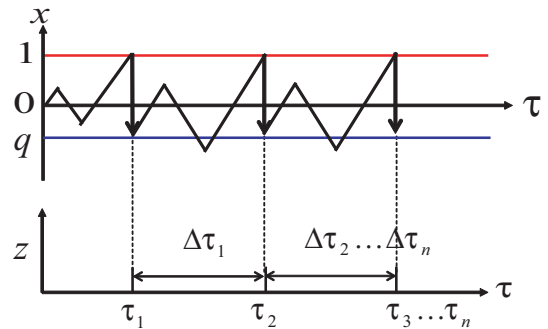


Figure 4: ISI definition

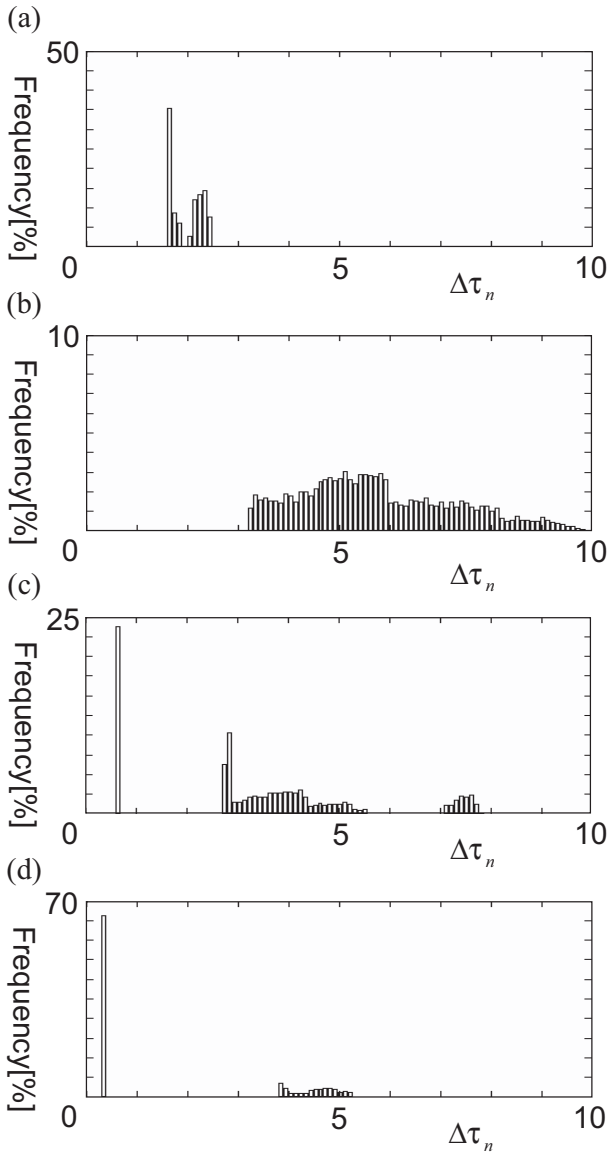


Figure 5: Histograms of ISI for  $a = 5$ . (a)  $q = -0.7$ , (b)  $q = 0$ , (c)  $q = 0.4$ , (d)  $q = 0.7$ .

can switch between  $q$  and 1 without rotation around the origin. It causes ISI of  $1 - q$  that appears in histogram in Fig. 5 (c). As  $q$  approaches 1, the ISI of  $1 - q$  becomes dominant as shown in Fig. 5 (d). Fig. 6 shows bifurcation of ISI ( $\Delta\tau_n$ ) for parameter  $q$ . As  $q$  approaches zero, the ISIs tend to be long and the distribution becomes to have wide band.

We can see that the ISI bifurcation diagram exhibits step-wise shape. This is because the maximum swing number between two-successive switching changes depending on  $q$ .

Fig. 7 shows attractors and histograms in windows in Fig. 6 ((a) and (b)). There are many windows in bifurcation diagram for  $q > 0$ . In the window, the system exhibits narrow chaotic attractors having ISIs concentrated in

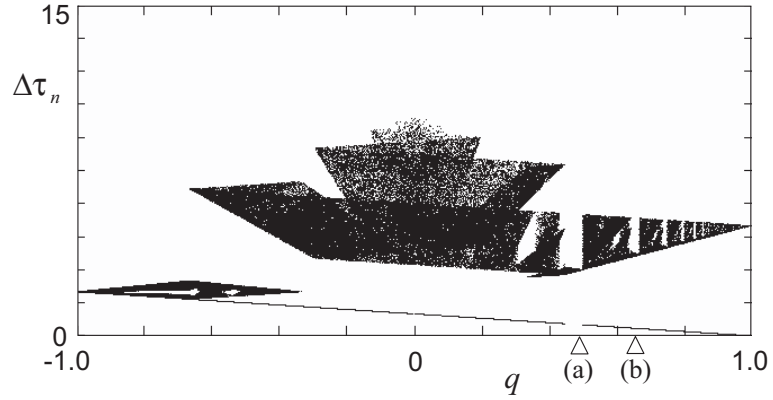


Figure 6: Bifurcation phenomena for  $a = 5$ .

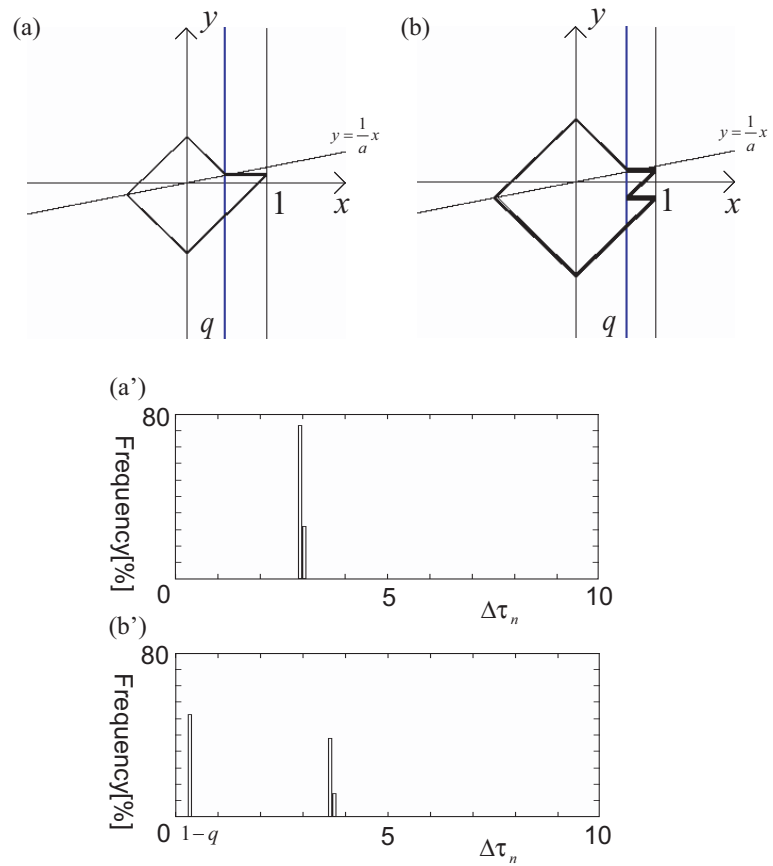


Figure 7: Attractors and histograms in windows for  $a = 5$ . (a) and (a')  $q = 0.49$ , (b) and (b')  $q = 0.65$ .

narrow-band(s) as shown in Fig. 7. Behavior of attractors in windows are chaotic, but it's ISI characteristics is very locally.

#### 4. Conclusions

We have presented the PWC-CSO and have analyzed its chaotic spike-trains. Since the vector field is PWC, the

trajectory is PWL and precise analysis is possible. We have investigated ISI characteristics and bifurcation phenomena: the system exhibits various chaotic spike-trains that cause interesting window-like structure in the bifurcation diagram. Future problems include theoretical analysis of ISI bifurcations and engineering applications.

### References

- [1] Y. Matsuoka and T. Saito, "A Simple Chaotic Spiking Oscillator Having Piecewise Constant Characteristics", *IEICE Trans. Fundamentals*, 89, 9, pp. 2437-2440, 2006.
- [2] K. Mitsubori and T. Saito, "Dependent switched capacitor chaos generator and its synchronization", *IEEE Trans. Circuits Syst. I*, 44, 12, pp. 1122-1128, 1997.
- [3] Y. Takahashi, H. Nakano and T. Saito, "A Simple Hyperchaos Generator Based on Impulsive Switching", *IEEE Trans. Circuits Syst. II*, 51, 9, pp. 468-472, 2004.
- [4] H. Nakano and T. Saito, "Grouping synchronization in a pulse-coupled network of chaotic spiking oscillators", *IEEE Trans. Neural Networks*, 15, 5, pp. 1018-1026, 2004.
- [5] S. R. Campbell, D. Wang and C. Jayaprakash, "Synchrony and desynchrony in integrate-and-fire oscillators", *Neural computation*, vol. 11, pp. 1595-1619, 1999.
- [6] T. Stojanovski, L. Kocarev and U. Parlitz, "Driving and synchronizing by chaotic impulses", *Phys. Rev. E*, 54, pp. 2128-2131, 1996.
- [7] G. M. Maggio, N. Rulkov and L. Reggiani, "Pseudo-Chaotic Time Hopping For UWB Impulse Radio", *IEEE Tran. Circuits Syst., I*, 48, 12, pp. 1424-1435, 2001.
- [8] H. Hamanaka, H. Torikai and T. Saito, "Quantized Spiking Neuron with A/D Conversion Functions", *IEEE Tran. Circuits Syst., II*, 53, 10, pp. 1049-1053, 2006.
- [9] T. Tsubone, T. Saito and W. Schwarz, "Probability distribution of the switching intervals in chaotic pulse stream - a comparative study", *Proc. of IEEE/ISCAS*, pp. 471-474, 1999.